International Journal of Rotating Machinery
1997, Vol. 3, No. 4, pp. 239–247
Reprints available directly from the publisher
Photocopying permitted by license only

Investigation of the Flow in Pelton Turbines and the Influence of the Casing

HEINZ-BERND MATTHIAS[a], JOSEF PROST[a,*] and CHRISTIAN ROSSEGGER[b]

[a] *Institute for Waterpower and Pumps, Vienna University of Technology, Karlsplatz 13, 1040 Wien, Austria;*
[b] *Ingersoll Dresser Pumps, Industriestraße B Nr.6, 2345 Brunn/Geb, Austria*

(Received 25 March 1997; In final form 11 April 1997)

At the institute for waterpower and pumps at the University of Technology Vienna we do a lot of research work observing the flow in the casing and the buckets of Pelton turbines. One interest of our research is to find criteria to estimate the influence of the splash water distribution in the casing on the turbine efficiency. Knowing the splash water distribution it is further possible to develop methods to provide visual documentation of the flow in and around the buckets from the beginning to the end of interaction.

Our measurements have been done on a single jet Pelton turbine with a runner pitch diameter of 420 mm. Our research shows that the casing has great influence to the operation of a Pelton turbine and so it is very important to include the casing as an important factor in all investigations. Aluminum honeycombs have been successful to bring the splashing water under control and to make good visual documentations of the flow.

Keywords: Flow in Pelton turbines, Influence of the casing, Visual documentation, Outline of the casing, Turbine efficiency

1. INTRODUCTION

At the test rig for Pelton turbines at the Institute for Waterpower and Pumps all kinds of operating conditions can be researched. A main interest of our research is to observe the flow in the casing of the turbine and to find criteria to estimate the influence of the splash water distribution in the casing on the turbine efficiency. Knowing the splash water distribution it is further possible to develop methods to provide visual documentation of the flow in and around the buckets from the beginning to the end of interaction.

2. THE TEST RIG

At our test rig the research of multi-jet Pelton turbines with a pitch diameter up to 500 mm by heads up to 260 m is possible. The head for the turbine is produced by three pumps (parallel and/ or serial operation). They are powered by speed

* Corresponding author. Tel.: +43 1 58801-3211. Fax: +43 1 504 1148.

regulated DC-motors, which allow an optimal adjustment of the pumps with respect to the head and flow of a defined operation point of the Pelton turbine.

The DC-motor-generator for the Pelton turbine allows a real 4-quadrant operation. He can be regulated by speed or current and has the following characteristics:

$$P = 87\,\mathrm{kW},$$
$$n = \pm 0\text{--}3000\,\mathrm{min}^{-1}.$$

To measure the frictional force the turbine shaft is equipped with a hydrostatic bearing. The shaft is connected with the DC-motor-generator by an RSG-torquemeter and a gearing.

All kinds of data are recorded by electromechanical measuring instruments. The output signals of the amplifiers are digitized. So the measured data can be treated by a personal computer. For more details of the test rig see Rossegger *et al.* (1990) or Rossegger (1991).

The reported measurements have been done on a single jet Pelton turbine with a runner pitch diameter of 420 mm.

3. SPLASH WATER DISTRIBUTION IN A RECTANGULAR CASING

To get basic knowledge of the flow distribution the first tests were made with a rectangular casing with transparent walls, see Fig. 1. The only installations were a splash-guard to protect the wall opposite to the nozzle and a bucket-plate to reduce the splash water in the upper part of the casing.

Photos and videos were made and analyzed. An important factor to get usable pictures was the position of the camera and optimal illumination conditions (brightness, position of the lamps). The shutter speed of the camera system was controlled by the generator speed.

For the given geometric and hydraulic configuration we found four criteria to classify the flow

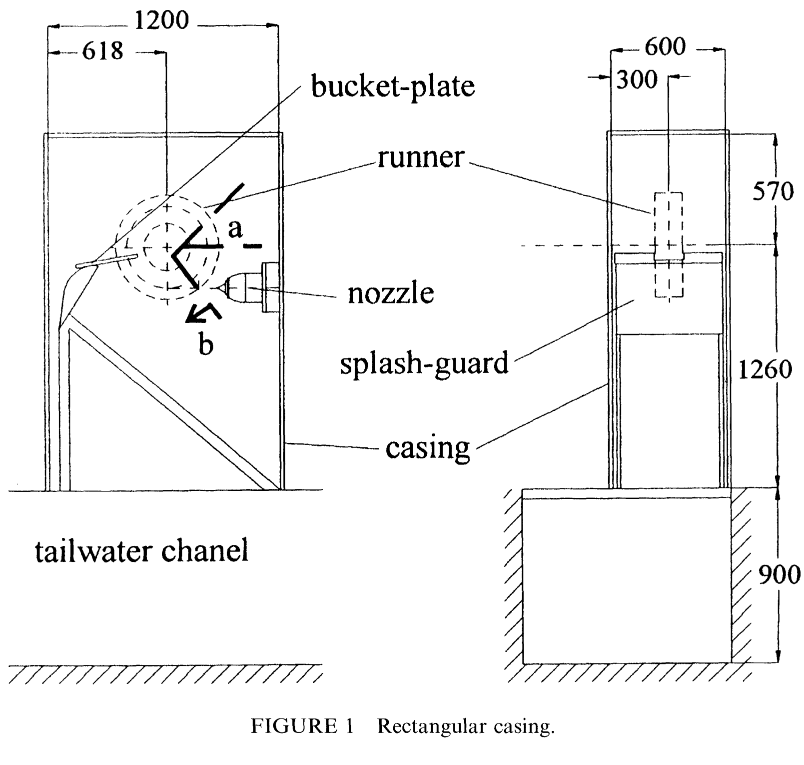

FIGURE 1 Rectangular casing.

distribution (Wurm, 1990):

(1) *Classification of the splash water distribution by observing how the normal projection of the Pelton runner to the casing is covered by splash water*. The splash water distribution at the transparent wall of the casing can be classified into four groups, which are dependent on the operation point of the turbine:
   - *Group 1* (Fig. 2(a)) is independent of the flow and can only be observed at low generator speed. It shows the trend from the optimal operation point to low unit speed.
   - *Group 2* (Fig. 2(b)) is independent of the flow and can only be observed in the optimal range of operating conditions. It shows the trend from the optimal operation point to high unit speed.
   - *Group 3* (Fig. 2(c)) is dependent on the flow and is located above the optimal range of operating conditions.
   - *Group 4* is the field near and above the runaway speed of the turbine. No covering of the turbine with splash water can be observed in this field.

(2) *Angle of contact of the splash water to the casing*. The angle of contact ('a' in Fig. 1) is a function of the buckets geometry, the flow and the speed. In the optimal operation range the angle of contact gets to a minimum and is about 45–50°. Besides no lateral flow can be observed in the optimal operating range.

(3) *Area of flood in the casing*. Flood means that the water falls back from the casing to the runner and impinges on the runner at the rear of the buckets. This depends only on the geometry of the casing. In our case the water impinges on the vertical side walls of the casing, flows to the rear upper edge and is reflected there. In the turbine characteristic the area of flood is located at low unit speed and higher unit discharge.

(4) *Water transport around the circuit of the Pelton runner* ('b' in Fig. 1). The water transport is dependent on flow and generator speed and can be estimated to nearly 250° measured from jet contact. The point of full emptying of the bucket depends mainly on the unit speed.

4. INFLUENCE OF THE CASING TO THE PERFORMANCE OF THE TURBINE

The next step of our research work was the variation of the casing in order to analyze the influence of the casing to the performance of the turbine, (Rossegger, 1991). For the given geometrical and hydraulic configuration we did research on the flow in different dome-shaped and rectangular casings in the regular and off-design operation range of the turbine. Finally we made an analysis of the losses to determine a 'casing-efficiency'.

The tests were made on 9 different casings. Figure 3 shows one of the casings with cylindrical dome. The radius and the width of the dome have been varied. Figure 4 shows an example of a tested

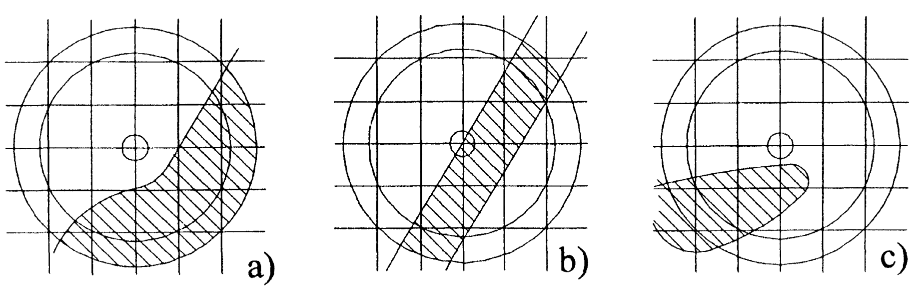

FIGURE 2 Splash water distribution at the wall of the rectangular casing.

casing with a rectangular dome. Modifications were made on the width of the dome.

Table I shows the list of the tested casings.

For each casing we determined the characteristic of the turbine. For a constant position of the needle of the nozzle and a constant head (constant unit discharge Q_{11}) the best efficiency point and the corresponding unit speed n_{11} can be located:

$$Q_{11} = \frac{Q}{D^2 \cdot \sqrt{H}}, \tag{1}$$

$$n_{11} = \frac{n \cdot D}{\sqrt{H}}. \tag{2}$$

The connecting line of these Q_{11}/n_{11}-values is the useful operation range of the turbine. The analysis shows that all lines (except the line of casing No. 121) are very close. The gradients rise sharply, the n_{11}-values range from 36.75 to 38 min^{-1} (from 37.2 to 38.3 min^{-1} for No. 121). So it seems to be permissible to use a mean unit speed of $n_{11} = 37.5\,\text{min}^{-1}$ for the further considerations.

For this value of n_{11} the graph of η_T as a function of Q_{11} can be estimated. Figure 5 shows the graph

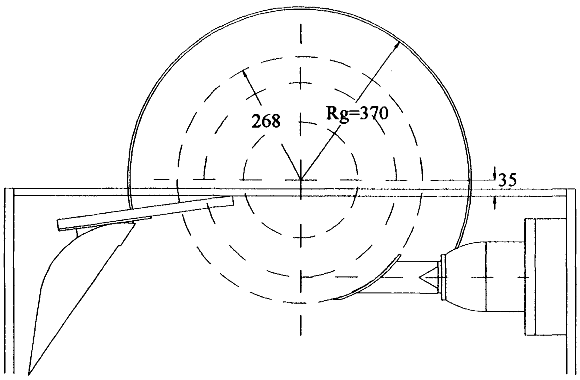

FIGURE 3 Casing with cylindrical dome.

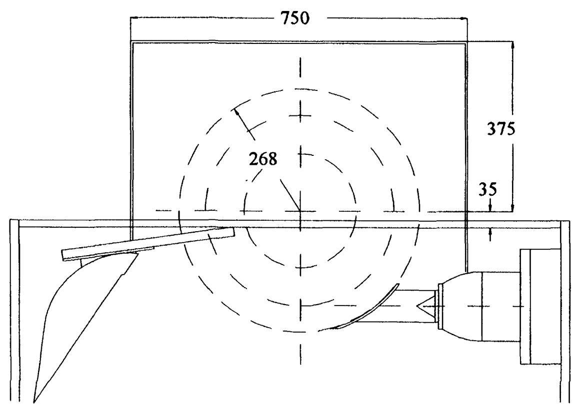

FIGURE 4 Casing with rectangular dome.

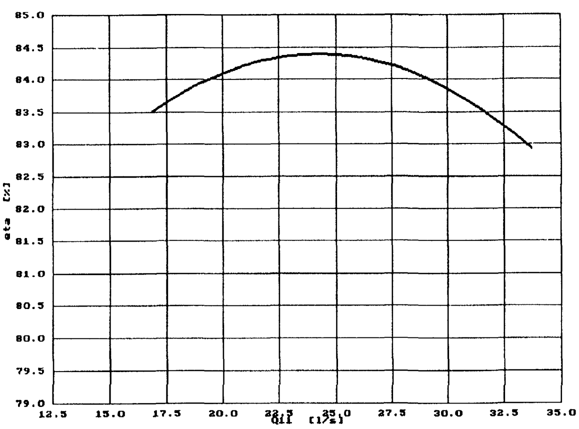

FIGURE 5 Efficiency versus unit discharge.

TABLE I Dimension of the tested casings

	Type	Width (mm)	Rg (mm)	Bucket-plate
No. 111	Cylindrical dome	150	275	Type A
No. 121	Cylindrical dome	235	275	Type A
No. 211	Cylindrical dome (Fig. 3)	150	370	Type A
No. 221	Cylindrical dome (Fig. 3)	235	370	Type A
No. 222	Cylindrical dome	235	370	Type B
No. 321	Rectangular dome (Fig. 4)	235	—	Type A
No. 322	Rectangular dome	235	—	Type B
No. 431	Rectangular casing (Fig. 1)	600	—	Type A
No. 430	Rectangular casing	600	—	—

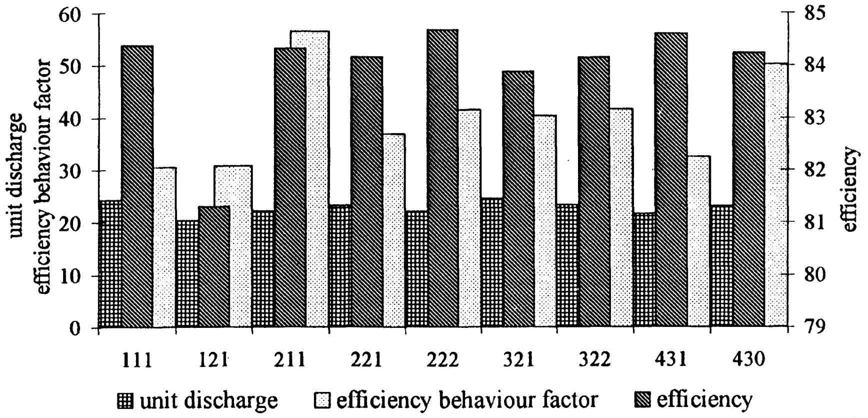

FIGURE 6 Effect of the casing on unit discharge, efficiency and efficiency behavior factor.

for casing No. 111. The best efficiency and the corresponding unit discharge now can be estimated. The results for all casings are presented in Fig. 6.

High values of Q_{11} are a result of a casing design which prevents flow to fall back into the runner. A good casing design for high Q_{11} is a casing with a very small slit between the wall and the runner (No. 111) or a casing with a great radial and axial expanse of the dome (No. 321). The so-called bucket-plate is useful for high Q_{11} too as water is disabled to enter the dome.

The turbine efficiency is nearly equal for each casing. Exception is the casing with a cylindrical dome with a small radial and a great axial slit (No. 121). Because of the great axial slit the dome of the casing is full of water which could not leave the dome. Although the best efficiencies of the other casings are almost the same the casings with cylindrical dome seem to be better as less water is in the casing. So the flow depends less on the reflections of the casing.

In order to rate the performance of the turbine in partial load and overload conditions (variation of discharge Q res. unit discharge Q_{11}) we defined an efficiency behavior factor. This factor is the radius of curvature at the vertex of the efficiency characteristic. High values of this factor mean high efficiency out of the optimum.

The determined factors are presented in Fig. 6. The casings with a small radius of the cylindrical dome (No. 111 and No. 121) have the minor efficiency behavior factor. Leaving the best efficiency point the efficiency of the turbine decrease rather quick. The best efficiency out of the optimum is detectable with casing No. 211 (small axial and great radial slit of the cylindrical dome).

At off design conditions (above and below the optimal unit speed) a significant change of the flow in the casing can be observed. Below the optimum of n_{11} there is more splash water in the casing because the relation of the geometry of the bucket and flow velocity is out of order. Above the optimum of n_{11} some part of the flow is no more involved in energy transformation and so there is less water in the upper casing parts. The determined best efficiencies at $n_{11} = 35\,\text{min}^{-1}$ and $n_{11} = 40.4\,\text{min}^{-1}$ are presented in Fig. 7. The behavior $\eta_T = f(Q_{11})$ represented by the efficiency behavior factor differs too, see Fig. 8.

5. ANALYSIS OF THE LOSSES

The losses in a Pelton turbine may be split up into the following losses:

- losses in the jet because of friction, high turbulence, jet-divergence and gravitation,
- losses in the runner because of friction in the buckets, entrance losses, . . . ,

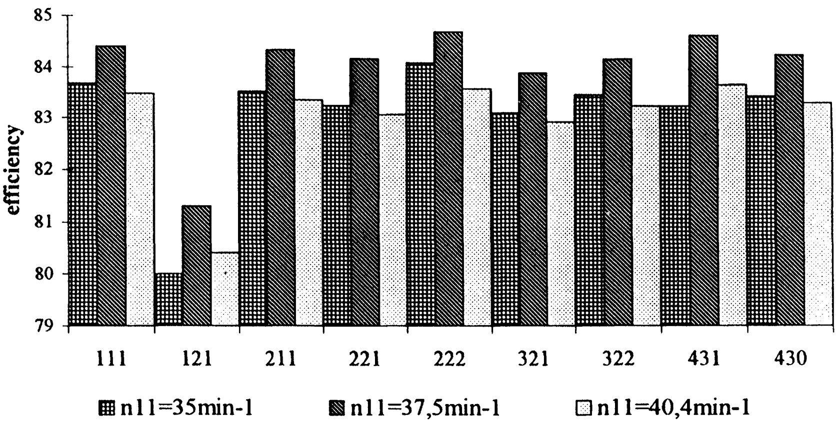

FIGURE 7 Effect of the unit speed on the efficiency.

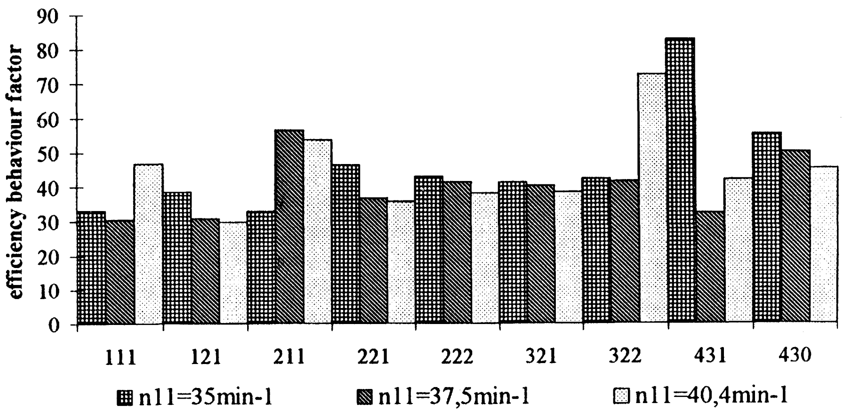

FIGURE 8 Effect of the unit speed on the efficiency behavior factor.

- losses in the casing because of ventilation and splash water falling into the runner and/or the jet,
- mechanical losses in the generator, bearings,...

In our investigation we only have to recognize the system jet–runner–casing. The efficiency of the turbine can be determined from the turbine characteristic. The efficiency of the jet (res. of the nozzle) can be obtained knowing the velocity of the jet by measuring the jet diameter at a known discharge. We measured the diameter of the jet using a Digital Image Processing System (DIP). A good approximate value of the efficiency of the runner can be estimated from the geometry of the bucket and the velocity triangles at the inlet and the outlet. The losses in the bucket are considered using experience values published in literature (e.g. Raabe, 1970).

The losses in the nozzle and in the runner estimated in this way come to approximately 13.2%, see Fig. 9. The efficiency of the casing now can be estimated by

$$\eta_{\mathrm{C}} = \frac{\eta_{\mathrm{T}}}{\eta_{\mathrm{N}} \cdot \eta_{\mathrm{R}}}. \tag{3}$$

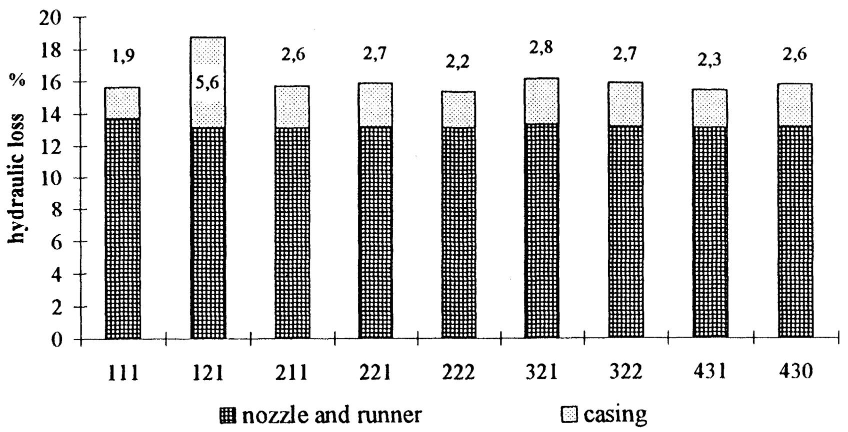

FIGURE 9 Efficiencies for the tested casings.

The efficiencies of the casings estimated in this way for $n_{11} = 37.5\,\mathrm{min}^{-1}$ are presented in Fig. 9. The values range from 1.9% to 2.8% except No. 121.

In summary it may be said that casing No. 211 seems to be the best compromise regarding efficiency and efficiency behavior both in design and off-design conditions. Other casings certainly show better efficiencies, but the efficiency behavior in some cases is much worse than in No. 211.

6. DOCUMENTATION OF THE FLOW IN THE BUCKET

Knowing the splash water distribution in the casing it seems obvious to use this knowledge for the visual documentation of the flow in the runner. Catching the splash water it is possible to make videos without reduction of quality. The rectangular casing (Fig. 1) was the basis.

For the regular catch and drain of the splashing water two elements with aluminum honeycombs were constructed (Eckert, 1993). The hexagonal grid made of thin aluminumfoils has the task to catch the splashing water from different directions without reflection of droplets. The function of the surrounding construction is the stable support of the honeycombs and the drain of the water. The element opposite to the shaft was narrow and adjustable in height (see Fig. 10). So the reduction of the view angle from the side can be minimized.

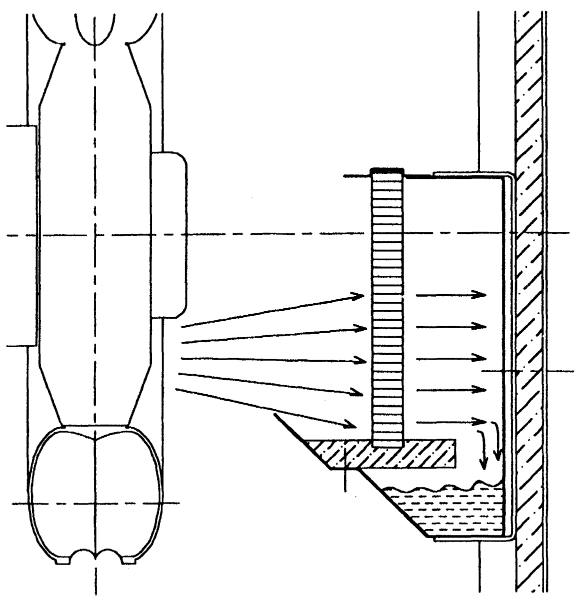

FIGURE 10 Catch of the splash water in the casing.

A normal 50 Hz video-camera with a tele-objective was used to observe from the outside through the open casing. There were two positions for the camera, see Fig. 11. To provide a stable image the stroboscopic light was triggered externally by an optical speed sensor. With the phase adjuster the image of the bucket could be adjusted by hand or moved continuously.

Figure 12 shows one example of the recorded pictures. You can see the entrance of the bucket into the jet and the flow in the bucket.

The stages of the beginning entrance of the bucket into the jet are visible in detail in Fig. 13.

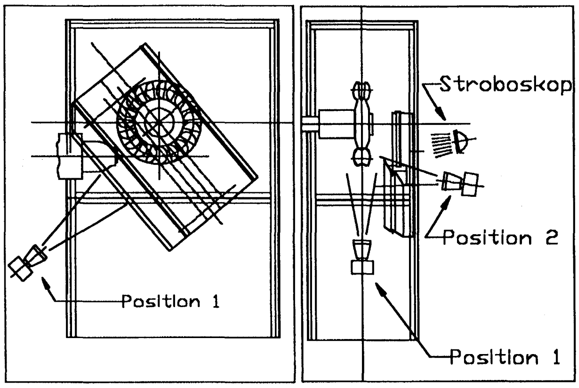

FIGURE 11 Positions for the camera.

In the upper left picture the outline of the jet is smooth. Drops of water are still leaving the bucket after a full rotation of the runner. When the tip of the bucket comes up to the jet the outline of the jet becomes rough. According with literature there are two possible reasons:

- The buckets have the effect of a radial compressor and the air leaving the runner interferes with the jet (Bachmann *et al.*, 1990).
- The drops coming out from the bucket slow down and dissolve the boundary surface of the jet (Grein, 1990).

Following there is a summary of the observed phenomena:

- Perturbation of the surface of the jet and separation of droplets when the cutout of the bucket approaches the jet (Fig. 13).
- Detachment of the jet by the bucket not in a clean matter; the cut off part of the jet tears off in a very irregular structure; the part adhering

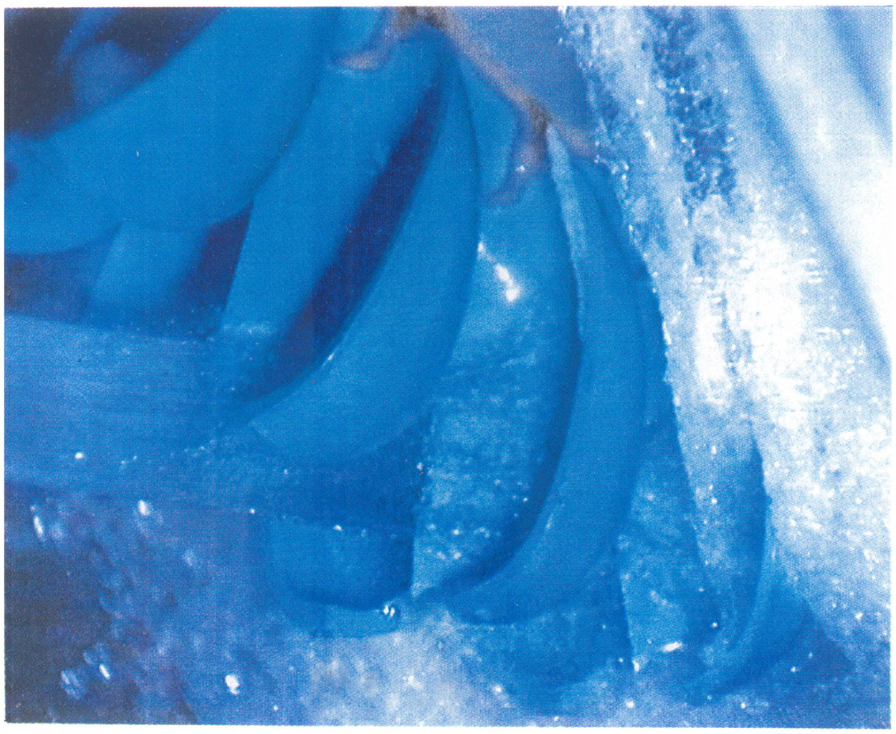

FIGURE 12 Flow in the buckets of a Pelton runner.

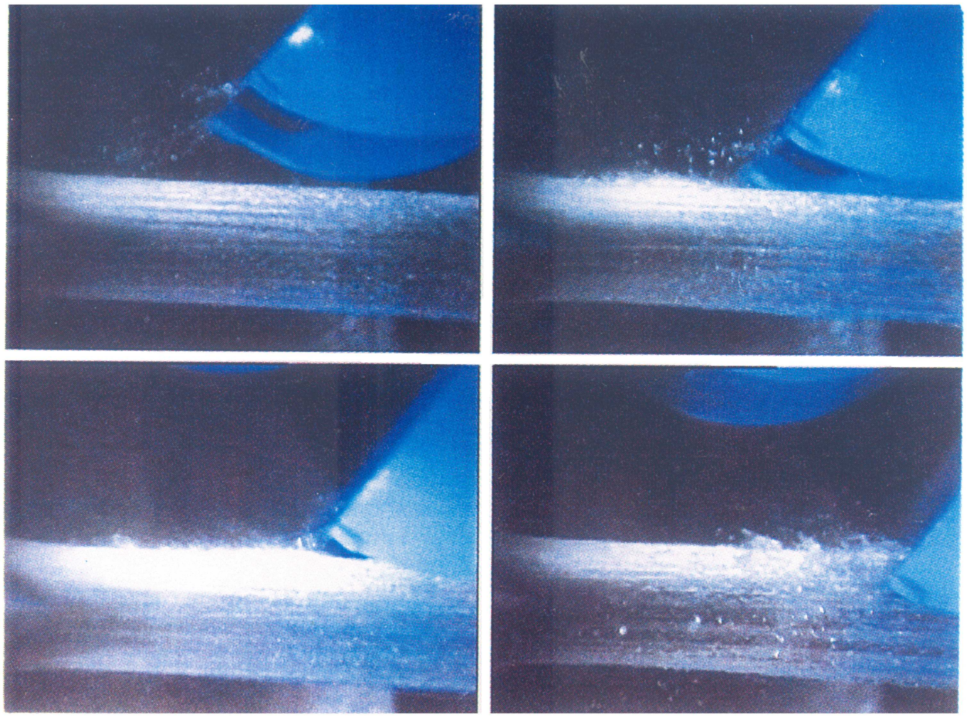

FIGURE 13 Entrance of the buckets into the jet.

on the backside of the bucket moves radial out of the runner.

- The flow out of the bucket forms sheets of water; the sheets fuse to a wall of splash water.
- Water from the cutout region on the backside of the bucket fans out towards the ribs of the bucket and splashes off.

NOMENCLATURE

Q_{11}	unit discharge, l/s (10^{-3} m^3/s)
n_{11}	unit speed, min^{-1}
Q	discharge, l/s (10^{-3} m^3/s)
H	head, m
D	pitch diameter, m
η_T	efficiency of the turbine, %
η_C	efficiency of the casing, %
η_N	efficiency of the nozzle (jet), %
η_R	efficiency of the runner, %

References

Bachmann, P. *et al.* (1990) Experimental flow studies on a 1-jet model Pelton turbine, *Proceedings of the 15th I.A.H.R. Symposium*, Vol. 2, Article R3.

Eckert, F. (1993) Realisierung und erste Anwendung eines Systems zur visuellen Dokumentation der Strömungsvorgänge in den Schaufeln einer Peltonturbine, Diploma thesis, Vienna University of Technology.

Grein, H. (1990) Cavitation pitting and rain erosion on Pelton runners, *Proceedings of the 15th I.A.H.R. Symposium*, Vol. 1, pp. H6.1–10.

Rossegger, Ch. *et al.* (1990) Computeraided measurement system for hydro turbines, *International Water Power & Dam Construction*, **42**(3), 28–33.

Rossegger, Ch. (1991) Ein Beitrag zur Untersuchung des Gehäuseeinflusses auf das Betriebsverhalten einer Modellpeltonturbine unter besonderer Berücksichtigung der Automatisierung des Versuchsstandes, Doctoral thesis, Vienna University of Technology.

Raabe, J. (1970) *Hydraulische Maschinen und Anlagen – Teil 2 Wasserturbinen*, VDI-Verlag, Düsseldorf.

Wurm, L. (1990) Dokumentation und Analyse verschiedenen Betriebszustände einer Peltonturbine, Diploma thesis, Vienna University of Technology.